Electronic Supplementary Material (ESI) for Journal of Materials Chemistry C.

Electronic Supplementary Information

Structure of MFU-4*l*

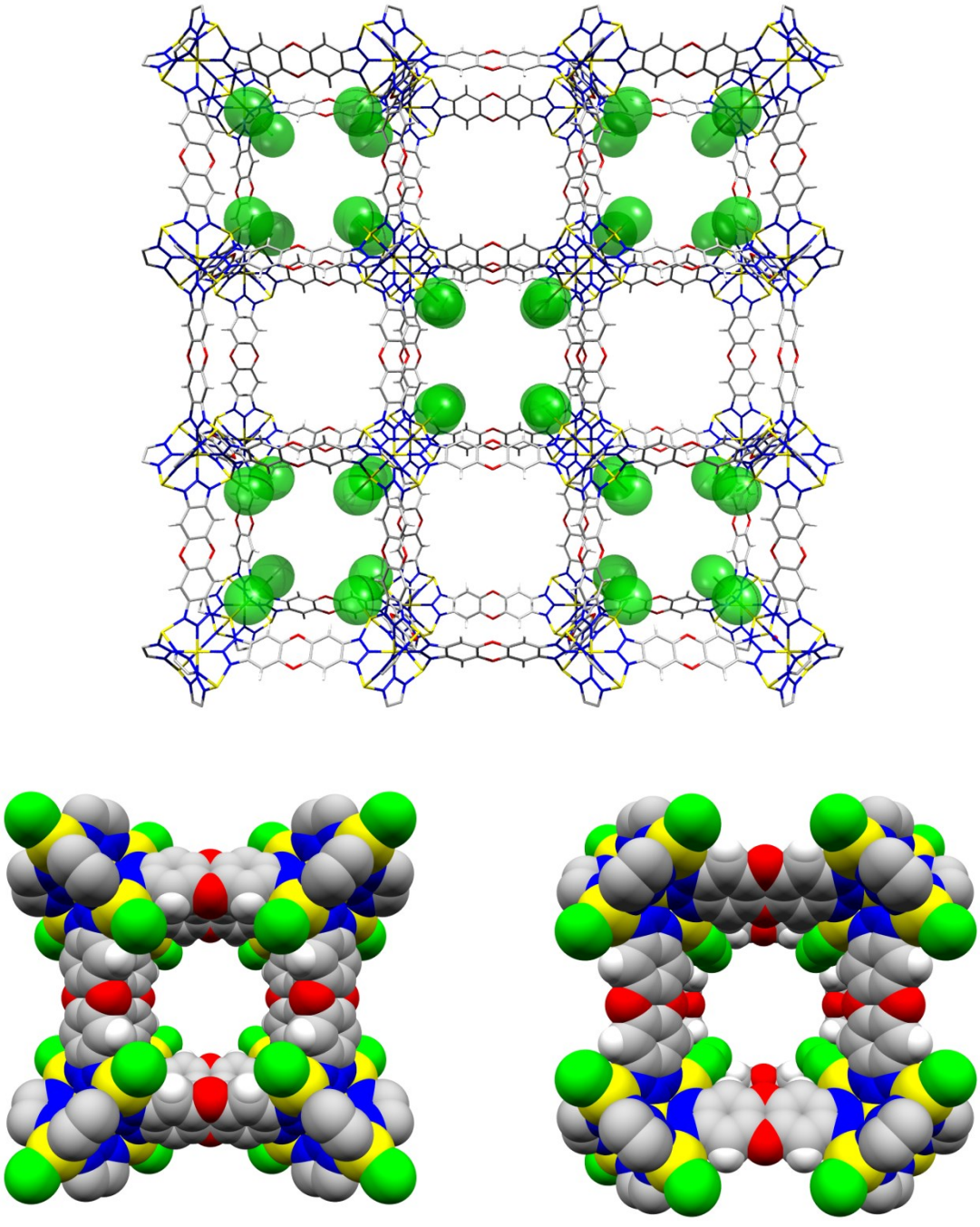

Figure S1: (top) Structure of MFU-4l evidencing the position of the chlorine atoms (bottom) Illustration of the 2 types of cages of MFU-4l with chlorine atoms pointing outside (left) and inside (right) the cavity. Color code: Zn=yellow, C=grey, N=blue, O=red, Cl=green, H=white.

Structure of MIL-100(Al)

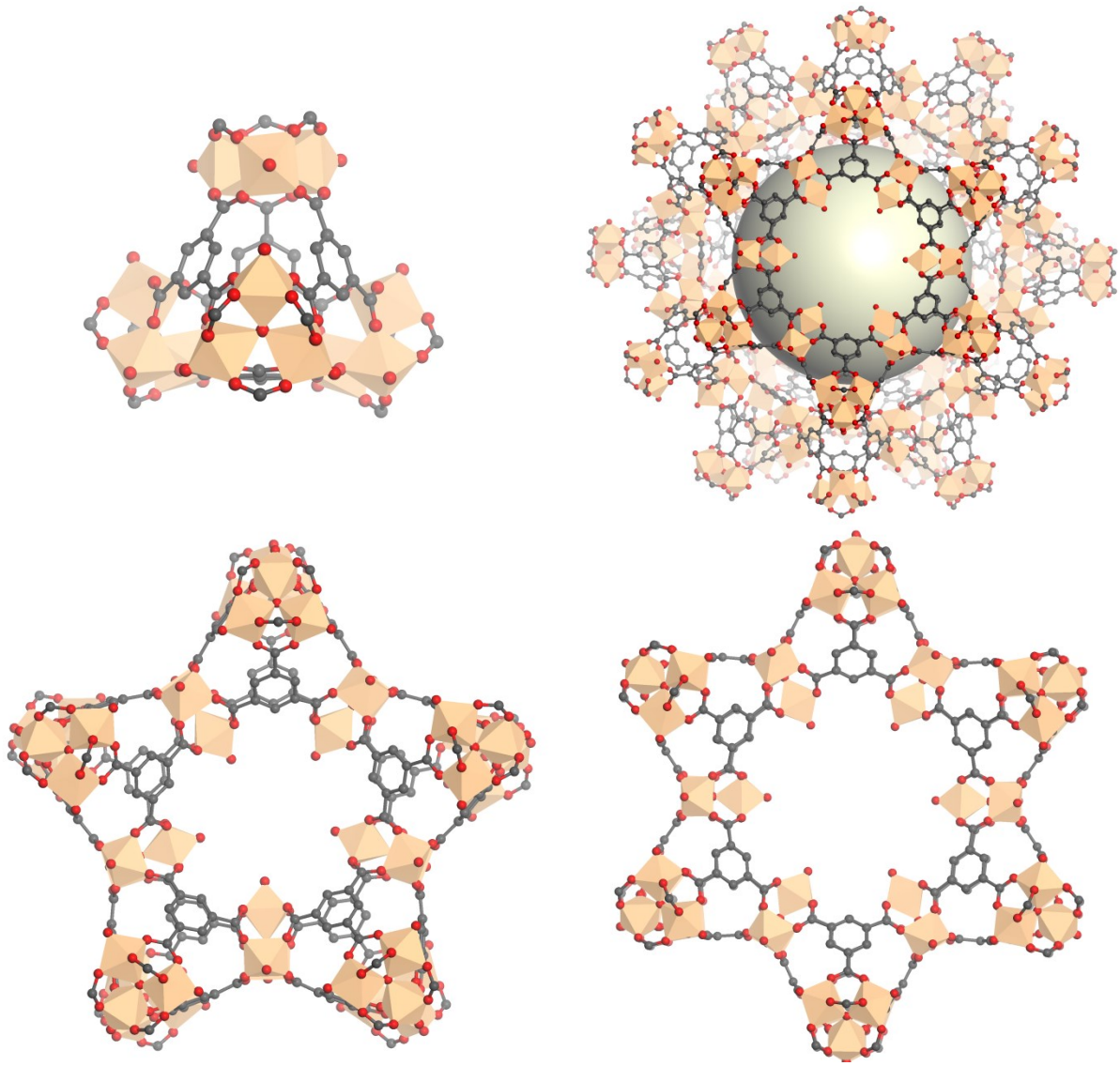

Figure S2: Structure of MIL-100(Al) (top left) Supertetrahedral building unit of the MOF built with Al oxocentered trimers and trimesic acid; (top right) Structure of the large cage of MIL-100(Al) (bottom left) Pentagonal window allowing to access the cage and (bottom right) Hexagonal window allowing to access the cage. Color code: Al=orange, C=grey, O=red. H atoms are omitted for clarity.

Determination of linker and Fe^{II} loading by EDS and liquid NMR.

NMR samples were prepared by digesting ca 3 mg of the MOF material with D_2SO_4/D_2O then dissolving the resulting suspension in $(CD_3)_2SO$.

MFU-4*l*: Starting from the bare MOF with formula $Zn_5(BTDD)_3Cl_4$ and a Zn/Cl ratio of 1.2 which was confirmed by EDS (Table S1 Zn/Cl ratio expected 1.25, measured 1.2).

Statistics	Cl (mol %)	Zn (mol %)
Max	49.4	56.8
Min	43.2	50.6
Average	45.4	54.6
Standard Deviation	2.1	2.1

Table S1. EDS Analysis of MFU-4l

BPI⊂MFU-4*l*:

^1H NMR analysis of the digested sample indicates a BTDD/BPI^- ratio of 1.5 (Figure S3), thus if every BPI^- linker substitutes a Cl^- anion from the SBUs, the expected formula is $Zn_5(BTDD)_3(BPI)_2Cl_2$, which is confirmed by EDS (Table S2, Zn/Cl ratio expected 2.5, measured 2.8). The electroneutrality of the structure is ensured as Cl^- anions are substituted by BPI^- anions from the BPI.Li salt.

Statistics	Cl (mol %)	Zn (mol %)
Max	28.1	75.3
Min	24.7	71.9
Average	26.2	73.8
Standard Deviation	1.3	1.3

Table S2. EDS Analysis of BPI⊂MFU-4l

1⊂MFU-4*l*:

^1H NMR analysis of the digested sample indicates a BTDD/(HBPI or BPI^-) ratio of 0.86 (Figure S3). BPI^- anions have been anchored on the previous step, while HBPI are capping the Fe(II) cations coordinated to the BPI^- anions in this step. Therefore, if we assume that one Fe(II) cation is anchored per previously grafted BPI^- linker, and that the electroneutrality is ensured by the loading of two ClO_4^- anions per Fe(II), we can propose the following formula: $Zn_5(BTDD)_3Cl_2[(BPI)_2Fe_2(HBPI)_{1.5}(ClO_4)_4]$.

EDS analysis (Table S3) indicates the following ratios: Zn/Fe ratio expected 2.5, measured 2.62, Zn/Cl ratio expected 0.83, measured 1.03, which are consistent with the proposed formula from NMR measurements. The slightly lower amount of Cl measured compared to the expected one might come from a partial deprotonation in solution of HPBI linker added in the last step that will balance the "missing" negative charge from the perchlorate.

Statistics	Cl (mol %)	Zn (mol %)	Fe (mol %)
Max	44.7	49.2	22.3
Min	36.0	33.1	10.2
Average	41.4	42.5	16.2
Standard Deviation	2.9	7.1	4.9

*Table S3. EDS Analysis of **1**⊂MFU-4l.*

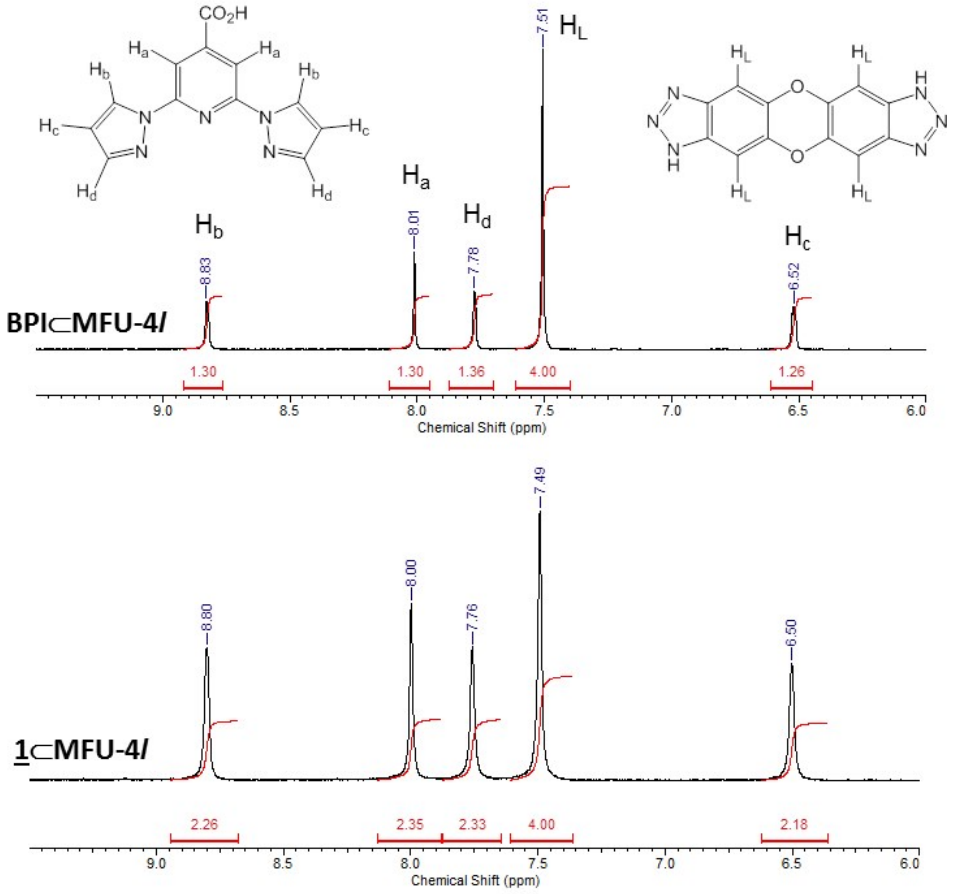

Figure S3. [1]H NMR spectra of acid digested samples of BPI⊂MFU-4l and 1⊂MFU-4l.

BPI⊂MIL-100(Al):

[1]H NMR analysis of the digested sample indicates a BTC/BPI$^-$ ratio of 3.3 (Figure S4), thus if every BPI$^-$ linker substitutes a OH$^-$ group from the SBUs, the expected formula is $Al_3O(OH)_{0.4}(H_2O)_2(BTC)_2(BPI)_{0.6}$. The electroneutrality of the structure is ensured as OH$^-$ anions are substituted by BPI$^-$ anions from the BPI.Li salt.

1⊂MIL-100(Al):

[1]H NMR analysis of the digested sample indicates a BTC/(HBPI or BPI$^-$) ratio of 1.8 (Figure S4). BPI$^-$ anions have been anchored on the previous step, while HBPI are capping the Fe(II) cations coordinated to the BPI$^-$ anions in this step. Therefore, if we assume that one Fe(II) cation is anchored per previously grafted BPI$^-$ linker, and that the electroneutrality is ensured by the loading of two ClO_4^- anions per Fe(II), we can propose the following formula: $Al_3O(OH)_{0.4}(H_2O)_2(BTC)_2[(BPI)_{0.6}Fe_{0.6}(HBPI)_{0.51}(ClO_4)_{1.2}]$.

EDS analysis (Table S4) indicates the following ratios: Al/Fe ratio expected 5, measured 2.9, Al/Cl ratio expected 2.5, measured 2.2, Therefore, an excess of iron is detected, while the amount of Cl is consistent with the proposed formula from NMR measurements. It can be

explained by a partial substitution of Al^{III} cations from the MOF framework by Fe^{III} during the metalation step. Indeed the direct treatment of MIL-100(Al) (50 mg) by a solution of $Fe(ClO_4)_2.xH_2O$ (20 mg) in EtOH (20 mL) over 16 h at room temperature followed by thorough washings affords the mixed-metal material MIL-100(Al/Fe) with formula $Al_{2.67}Fe_{0.33}O(OH)(H_2O)_2(BTC)_2$ where 1/8 th of Al^{III} from SBUs have been replaced by Fe^{III} (see Table S5). Therefore, we can propose the following formula $Al_{2.67}Fe_{0.33}O(OH)_{0.4}(H_2O)_2(BTC)_2[(BPI)_{0.6}Fe_{0.6}(HBPI)_{0.51}(ClO_4)_{1.2}]$ that fit both NMR and EDS measurements.

Statistics	Al (mol %)	Cl (mol %)	Fe (mol %)
Max	66.3	29.4	26.3
Min	44.4	16.7	14.0
Average	55.5	25.6	19.0
Standard Deviation	7.4	4.1	4.6

*Table S4. EDS Analysis of **1**⊂MIL-100(Al)*

Statistics	Al (mol %)	Fe (mol %)
Max	93.1	18.6
Min	81.5	6.9
Average	88.9	11.1
Standard Deviation	3.4	3.4

Table S5. EDS Analysis of MIL-100(Al/Fe)

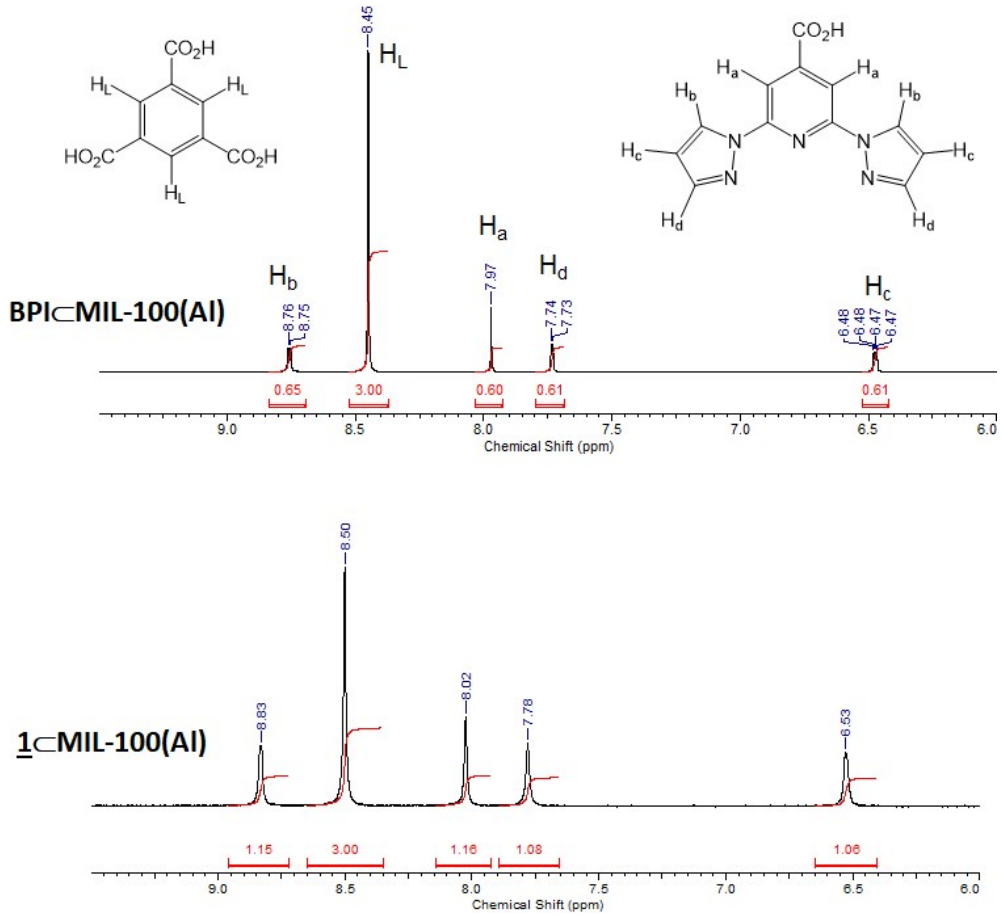

Figure S4. ^1H NMR spectra of acid digested samples of BPI⊂MIL-100(Al) and 1⊂MIL-100(Al).

Porosimetry

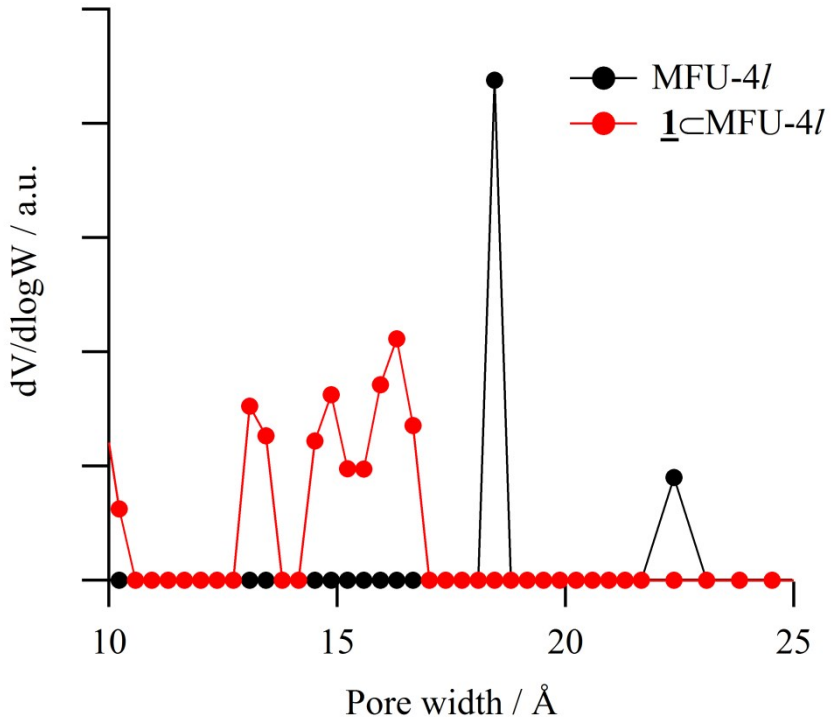

*Figure S5. Comparison of pore size distributions of MFU-4l and **1**⊂MFU-4l obtained by DFT*

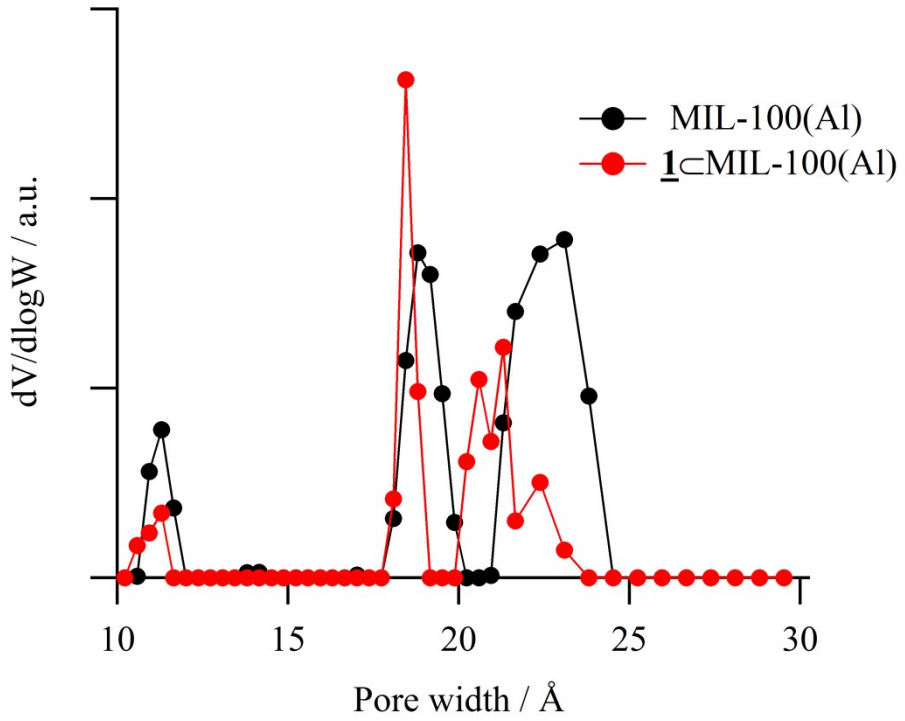

*Figure S6. Comparison of pore size distributions of MIL-100(Al) and **1**⊂MIL-100(Al) obtained by DFT*

Thermogravimetric analysis

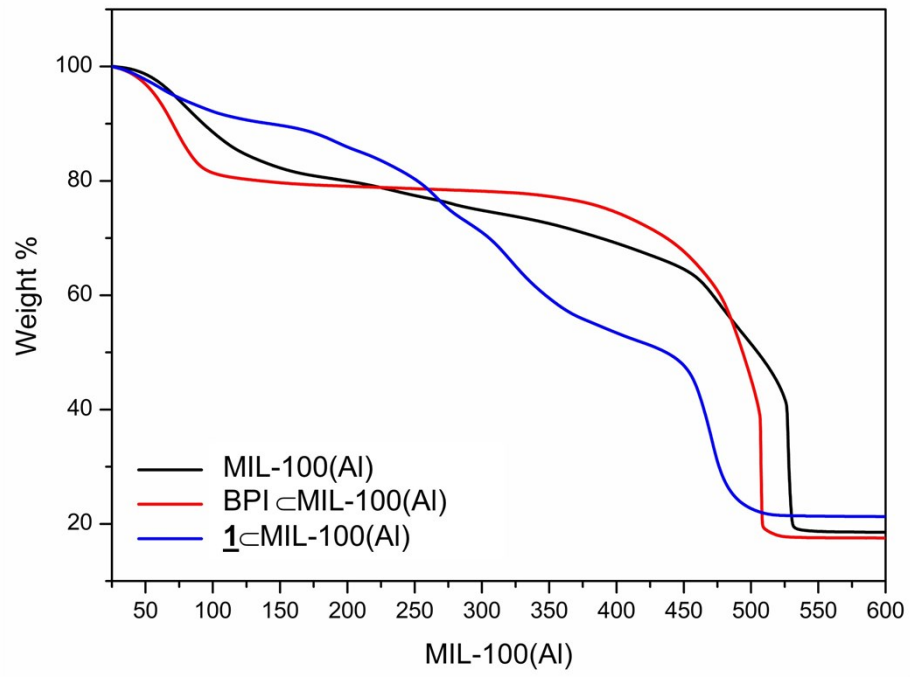

*Figure S7. Thermogravimetric analysis of MIL-100(Al), BPI⊂MIL-100(Al) and **1**⊂MIL-100(Al)*

Overall, the thermal stability of the compound is reduced during the functionalization. The weight loss corresponding to the departure of organic species (between 150 and 600°C) and the residue at 600°C have been compared to the formula proposed after NMR and EDS analysis (see before). The obtained results are in good agreement (less than 10% of deviation), which confirms the accuracy of the proposed formula.

MIL-100(Al):
Mass residue at 600°C (TGA): 18.5%
Formula at 600°C: $Al_3O_{4.5}$ (MW = 153 g.mol^{-1})
Mass residue at 300°C (TGA): 74.8%
Corresponding molecular weight (TGA): 618.6 g.mol^{-1}
Formula at 300°C (NMR): $Al_3O(OH)(H_2O)_2(BTC)_2$
Theoretical molecular weight: 564.2 g.mol^{-1}
Deviation: 9.6%

BPI⊂MIL-100(Al):
Mass residue at 600°C (TGA): 17.5%
Formula at 600°C: $Al_3O_{4.5}$ (MW = 153 g.mol^{-1})
Mass residue at 250°C (TGA): 78.2%
Corresponding molecular weight (TGA): 683.7 g.mol^{-1}
Formula at 250°C (NMR): $Al_3O(OH)_{0.4}(H_2O)_2(BTC)_2(BPI)_{0.6}$
Theoretical molecular weight: 706.0 g.mol^{-1}
Deviation: 3.3%

<u>1</u>⊂MIL-100(Al):
Mass residue at 600°C (TGA): 21.0%
Formula at 600°C (EDX): $Al_{2.67}Fe_{0.93}O_{5.4}$ (MW = 210.4 g.mol^{-1})
Mass residue at 100°C (TGA): 92.0%
Corresponding molecular weight (TGA): 921.8 g.mol^{-1}
Formula at 100°C (NMR): $Al_{2.67}Fe_{0.33}O(OH)_{0.4}(H_2O)_2(BTC)_2[(BPI)_{0.6}Fe_{0.6}(HBPI)_{0.51}(ClO_4)_{1.2}]$
Theoretical molecular weight: 998.6 g.mol^{-1}
Deviation: 7.7%

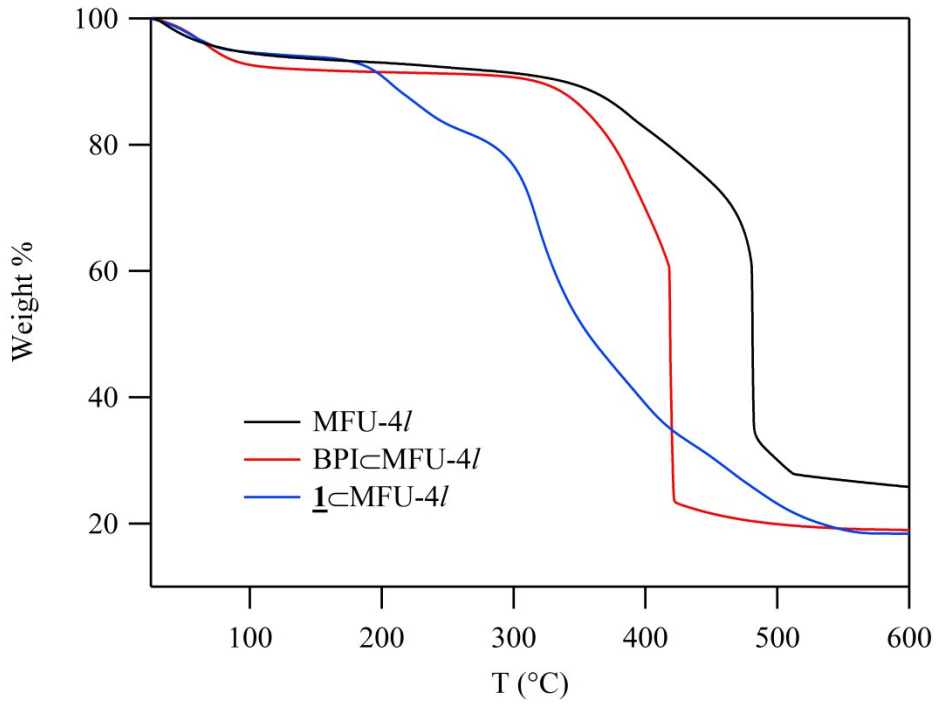

*Figure S8. Thermogravimetric analysis of MFU-4l, BPI⊂MFU-4l and **<u>1</u>**⊂MFU-4l*

Overall, the thermal stability of the compound is reduced during the functionalization. The weight loss corresponding to the departure of organic species (between 150 and 600°C) and the residue at 600°C have been compared to the formula proposed after NMR and EDS analysis (see before). The obtained results are in good agreement (less than 15% of deviation), which confirms the accuracy of the proposed formula.

MFU-4*l*:
Mass residue at 600°C (TGA): 25.9%
Formula at 600°C: Zn_5O_5 (MW = 407 g.mol^{-1})
Mass residue at 200°C (TGA): 92.9%
Corresponding molecular weight (TGA): 1460 g.mol^{-1}
Formula at 300°C (NMR): $Zn_5(BTDD)_3Cl_4$
Theoretical molecular weight: 1285.8 g.mol^{-1}
Deviation: 13.5%

BPI⊂MFU-4*l*:
Mass residue at 600°C (TGA): 19.0%
Formula at 600°C: Zn_5O_5 (MW = 407 g.mol^{-1})

Mass residue at 300°C (TGA): 90.7%
Corresponding molecular weight (TGA): 1942.9 $g.mol^{-1}$
Formula at 300°C (NMR): $Zn_5(BTDD)_3(BPI)_2Cl_2$
Theoretical molecular weight: 1723.6 $g.mol^{-1}$
Deviation: 12.7%

1⊂MFU-4*l*:
Mass residue at 600°C (TGA): 18.4%
Formula at 600°C: $Zn_5Fe_2O_8$ (MW = 566.6 $g.mol^{-1}$)
Mass residue at 150°C (TGA): 93.9%
Corresponding molecular weight (TGA): 2891.5 $g.mol^{-1}$
Formula at 150°C (NMR): $Zn_5(BTDD)_3Cl_2[(BPI)_2Fe_2(HBPI)_{1.5}(ClO_4)_4]$
Theoretical molecular weight: 2614.7 $g.mol^{-1}$
Deviation: 10.6%

Infrared spectroscopy

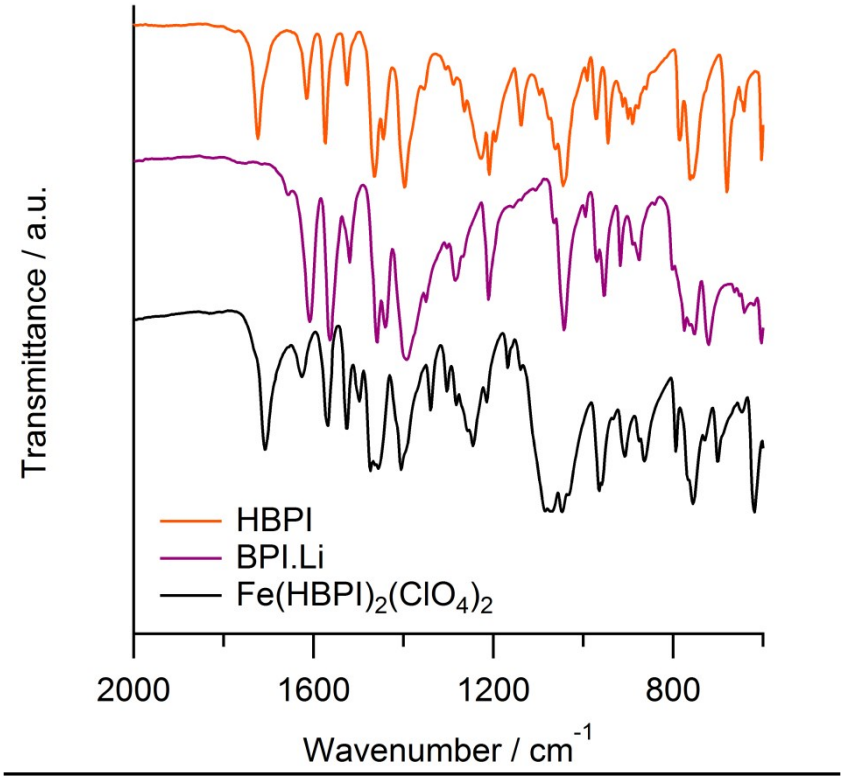

Figure S9. Infrared spectra of HBPI, BPI.Li and $Fe(HBPI)_2(ClO_4)_2$

HBPI	BPI.Li	$Fe(HBPI)_2(ClO_4)_2$	MFU-4*l*	**1**⊂MFU-4*l*	identification
1724	-	1708	-	1705	ν_{COOH} (stretching) of HBPI
-	-	-	1654	*	
1615	1608	1626	-	1625	$\nu_{C=N}$ (stretching) of BPI
1574	1563	1587	-	*	
-	-	-	1578	1572	
1526	1520	1526	-	1526	
1465	1459	1473	-	*	
-	-	-	1460	1459	
1445	1440	1456	-	*	
1397	1393	1405	-	1404	
-	-	-	1348	1349	
-	1284	-	-	-	
1227	-	-	-	-	
1209	1210	-	-	-	
-	-	-	1176	1175	
1139	-	-	-	-	
-	-	1070	-	1079	ν_{ClO4}
1045	1042	1045	-	1047	

HBPI	BPI.Li	$Fe(HBPI)_2(ClO_4)_2$	MIL-100(Al)	**1**⊂MIL-100(Al)	identification
1724	-	1708	-	1705	ν_{COOH} (stretching) of HBPI
-	-	-	1668	1669	
1615	1608	1626	-	1626	$\nu_{C=N}$ (stretching) of BPI
1574	1563	1587	-	1573	
1526	1520	1526	-	1525	
-	-	-	1465	1460	
1465	1459	1473	-	1460	
1445	1440	1456	-	1460	
-	-	-	1401	1403	
1397	1393	1405	-	*	
-	1284	-	-	-	
1227	-	-	-	-	
1209	1210	-	-	-	
1139	-	-	-	-	
-	-	1070	-	1080	ν_{ClO4}
1045	1042	-	-	-	
-	-	-	1045	1046	

*Table S6. Selected values of vibration bands (in cm^{-1}) of HBPI, BPI.Li, $Fe(HBPI)_2(ClO_4)_2$, MFU-4l, **1**⊂MFU-4l, MIL-100(Al) and **1**⊂MIL-100(Al). The bands noted * in **1**⊂MFU-4l and **1**⊂MIL-100(Al) are not detected because of overlaps with more intense bands of the MOF or **1**.*

UV-Visible spectroscopy

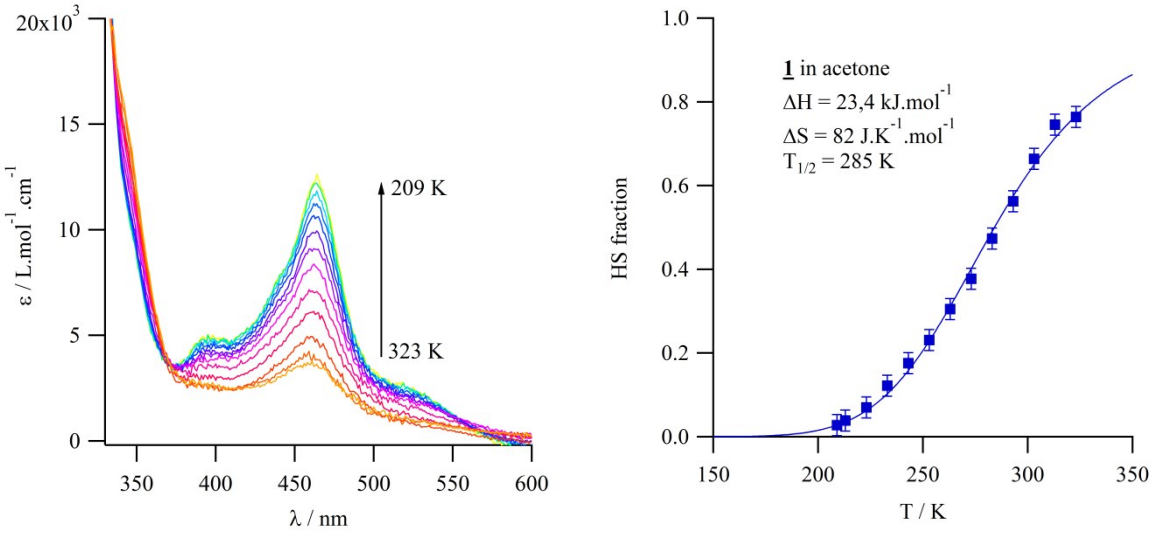

*Figure S10: (left) Temperature dependent UV-Visible spectra of **1** in acetone and (right) thermal spin crossover curve extracted from the UV-Visible spectra following the evolution of the absorption at 463 nm (maximum of the MLCT absorption band).*

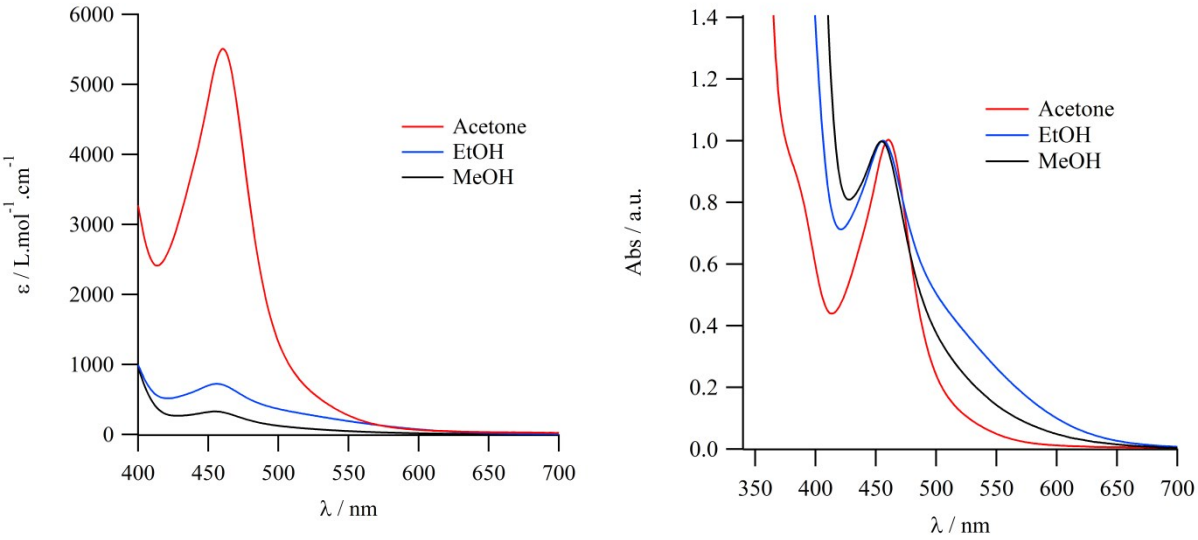

Figure S11: Absorption spectra of solutions containing $Fe(ClO_4)_2$ and ca. 8 equivalents of HBPI in different solvents.

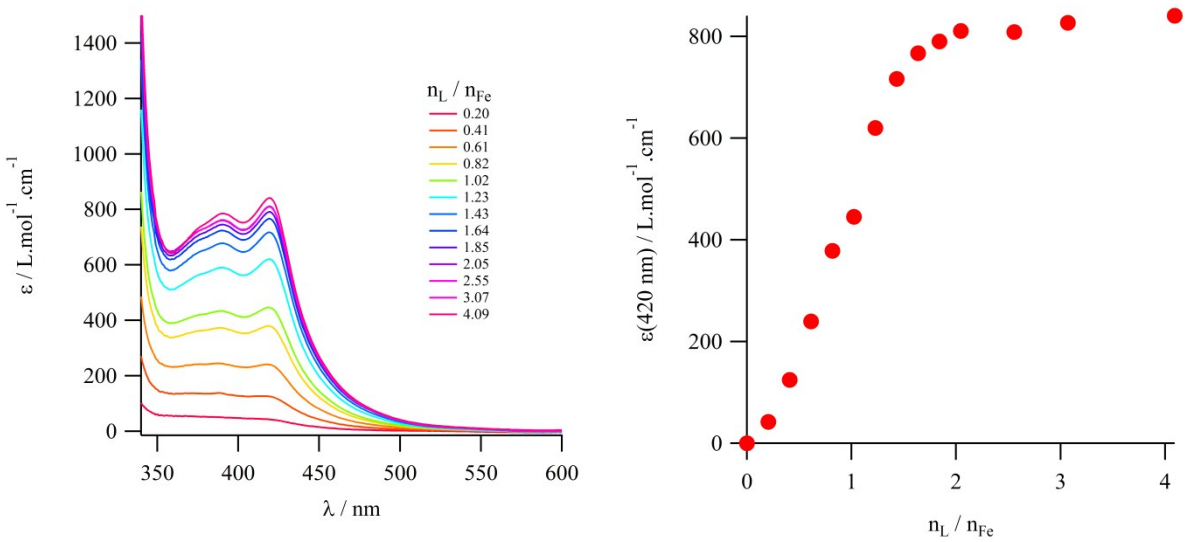

Figure S12: (left) Absorption spectra of a solution of $Fe(ClO_4)_2$ in acetone (0.218 mmol/L) in presence of different amounts of 1-BPP linker (right) Evolution of the molar extinction coefficient at 420 nm (maximum of the MLCT absorption band) as function of the amount of 1-BPP added.

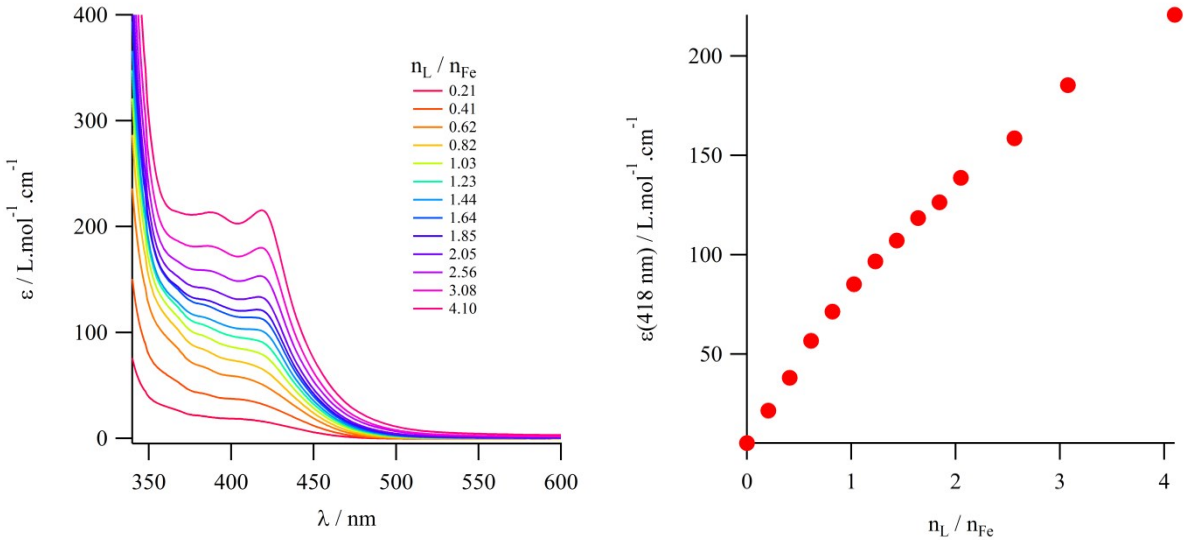

Figure S13: (left) Absorption spectra of a solution of $Fe(ClO_4)_2$ in EtOH (2.39 mmol/L) in presence of different amounts of 1-BPP linker (right) Evolution of the molar extinction coefficient at 418 nm (maximum of the MLCT absorption band) as function of the amount of 1-BPP added.

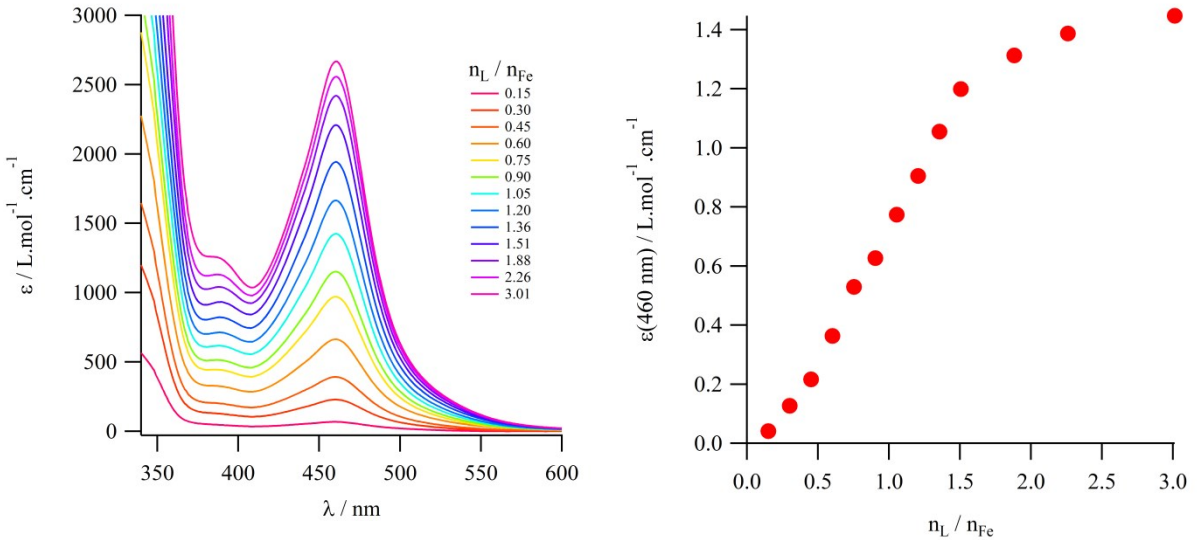

Figure S14: (left) Absorption spectra of a solution of $Fe(ClO_4)_2$ in acetone (0.261 mmol/L) in presence of different amounts of HBPI linker (right) Evolution of the molar extinction coefficient at 460 nm (maximum of the MLCT absorption band) as function of the amount of HBPI added.

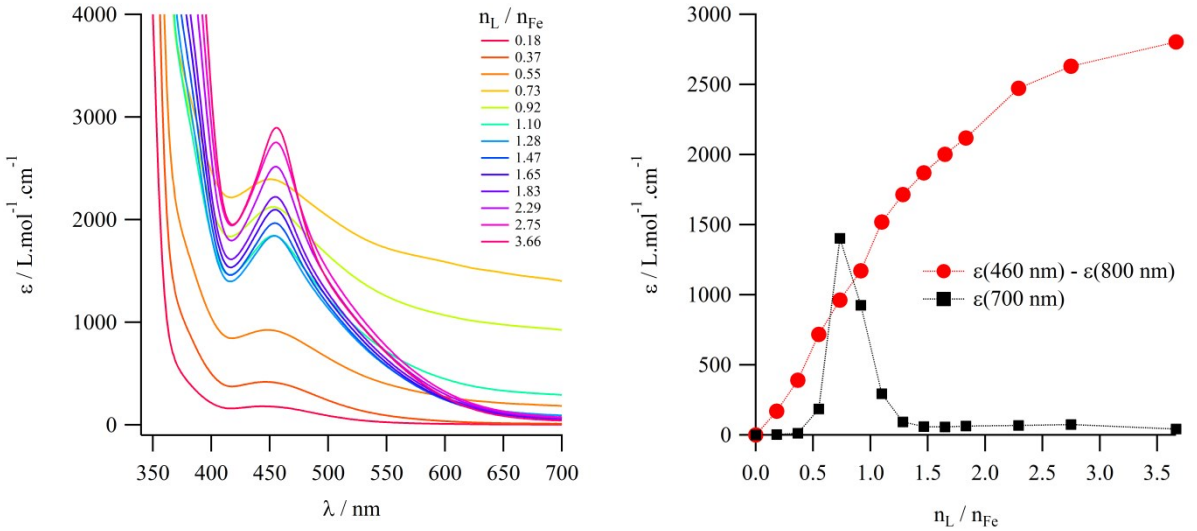

Figure S15: (left) Absorption spectra of a solution of $Fe(ClO_4)_2$ in EtOH (2.39 mmol/L) in presence of different amounts of HBPI linker. The jump in baseline around $n_L/n_{Fe} = 1$ is due to the precipitation of a red powder. (right) Evolution of the molar extinction coefficient at 700 nm (baseline jump) and of the difference between the molar extinction coefficient at 460 nm (maximum of the MLCT absorption band) and at 700 nm as function of the amount of HBPI added.

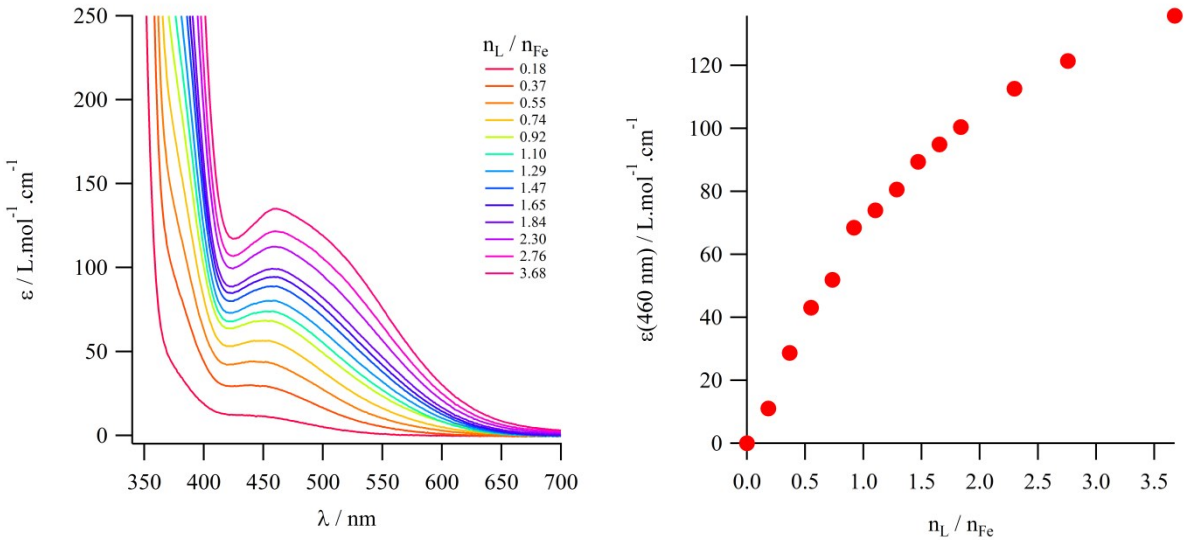

Figure S16: (left) Absorption spectra of a solution of $Fe(ClO_4)_2$ in EtOH (0.453 mmol/L) in presence of different amounts of HBPI linker (right) Evolution of the molar extinction coefficient at 460 nm (maximum of the MLCT absorption band) as function of the amount of HBPI added.

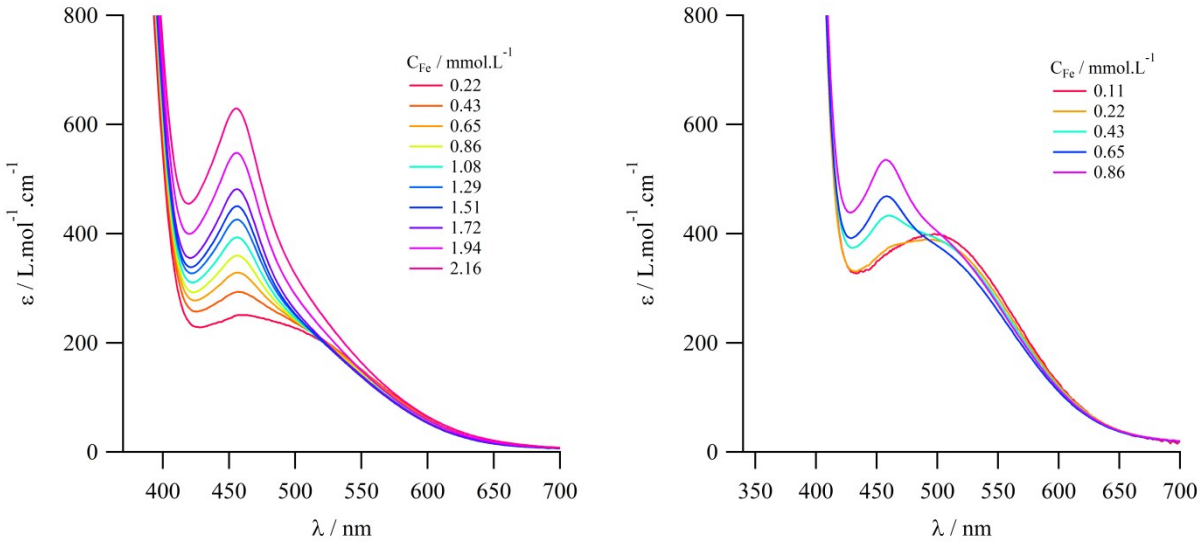

Figure S17: Absorption spectra of solutions containing $Fe(ClO_4)_2$ and HBPI in EtOH at different concentrations for a fixed molecular ratio between HBPI and Fe^{II} of 3.76 (left) and 14.6 (right).

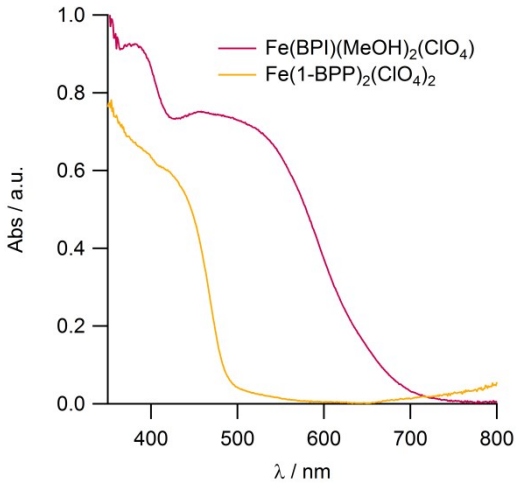

*Figure S18: Room-temperature solid state UV-Visible spectra of $Fe(1\text{-}BPP)_2(ClO_4)_2$ (High-Spin FeN_6 coordination sphere) and of **2** (High-Spin FeN_3O_4 coordination sphere)*

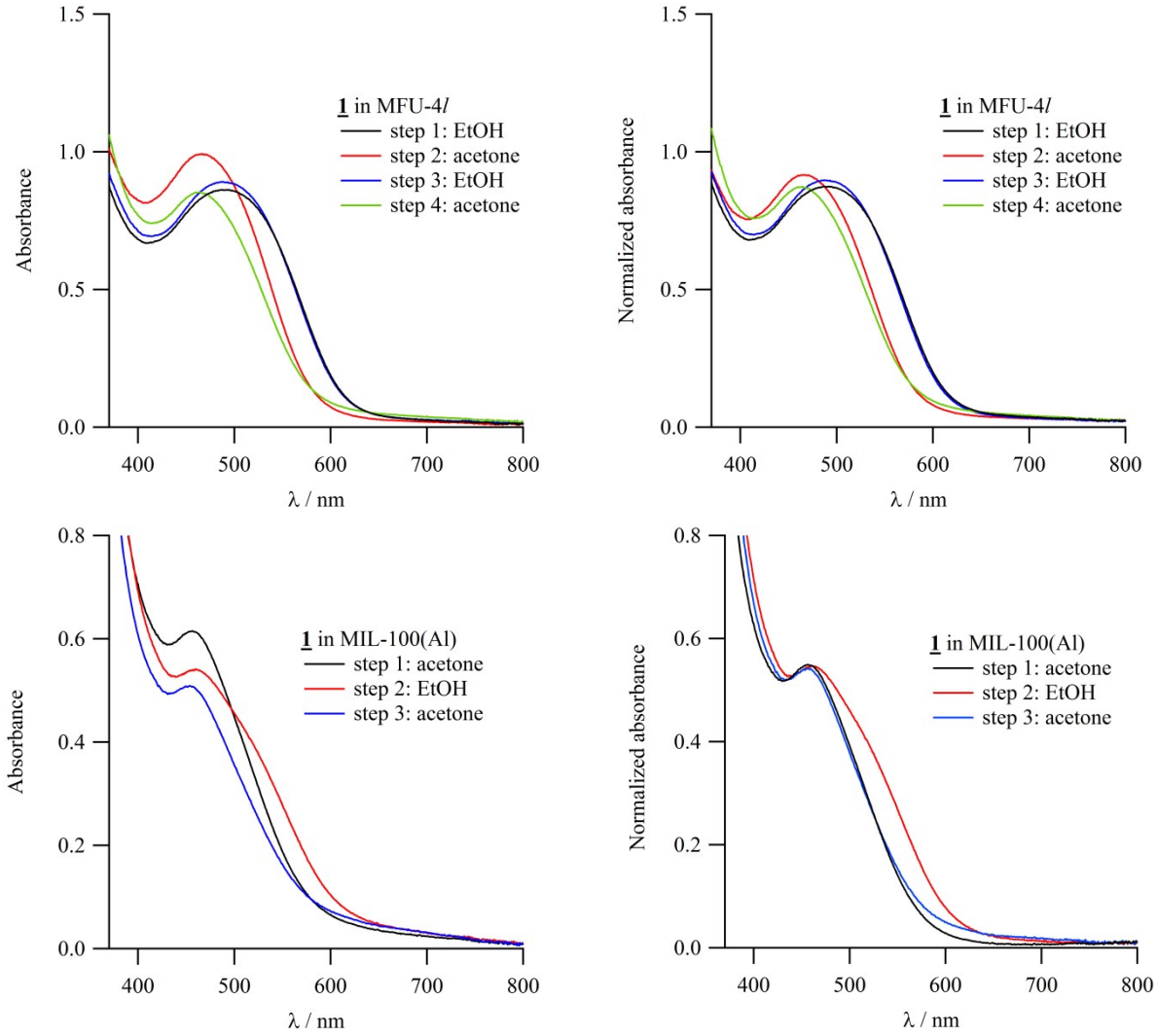

*Figure S19: UV-Vis spectra of **1**⊂MFU-4l without (top left) and with normalization (top right) and of **1**⊂MIL-100(Al) without (bottom left) and with normalization (bottom right) registered after several cycles of drying-redispersion of the solid performed sequentially in EtOH and acetone.*

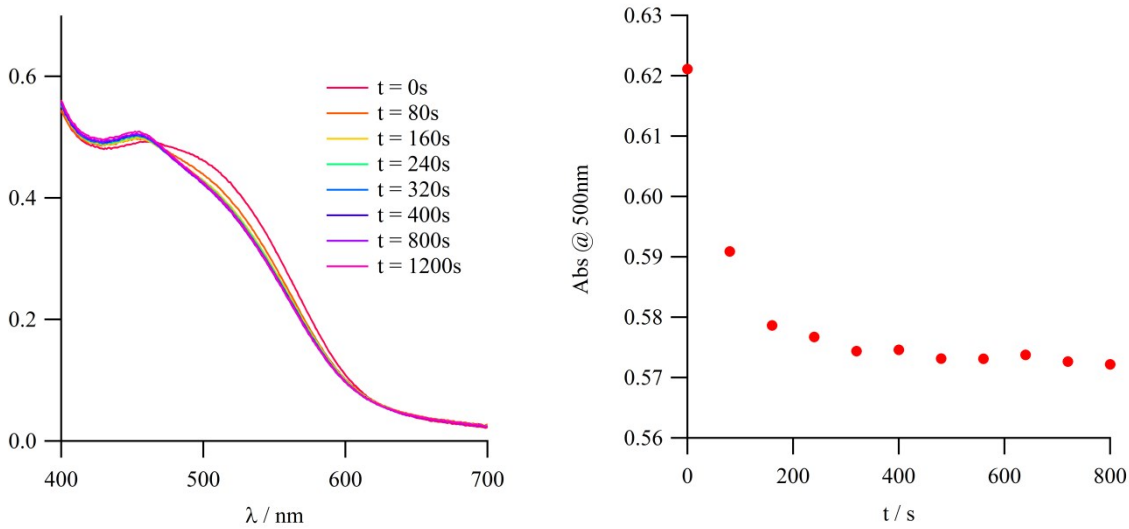

*Figure S20: UV-Vis spectra of **1**⊂MFU-4l in acetone-ethanol 3:1 solvent mixture after addition of 3 equivalents of acetone at t=0s on **1**⊂MFU-4l dispersed in pure ethanol (left) and Evolution of the absorbance at 500nm in acetone-ethanol 3:1 solvent mixture after the addition of acetone.*

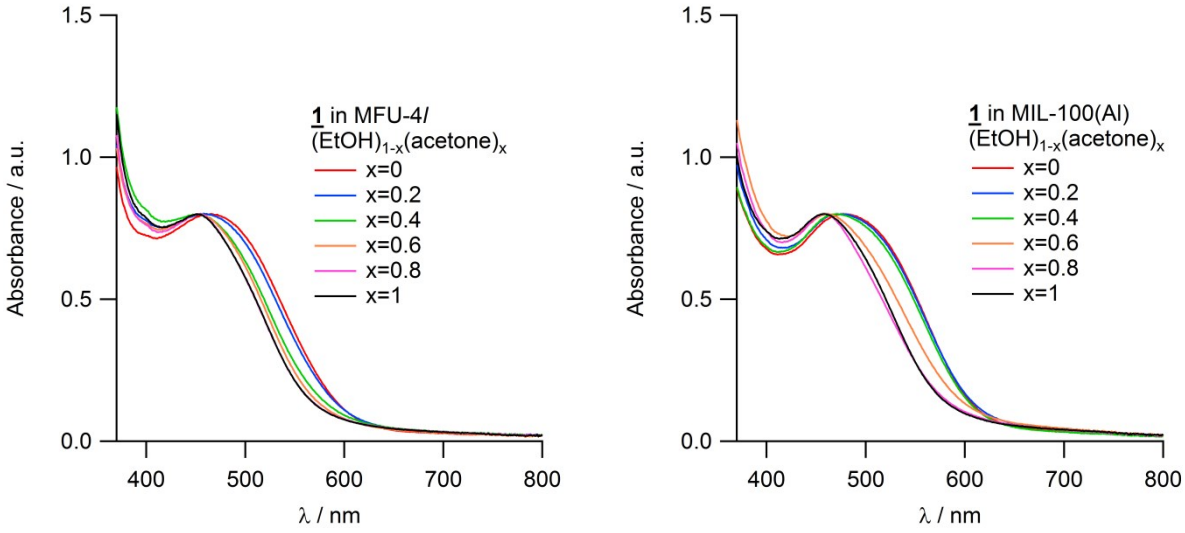

*Figure S21: UV-Vis spectra of **1**⊂MFU-4l(left) and **1**⊂MIL-100(Al) (right) in ethanol-acetone solvent mixtures*

Single-crystal X-Ray diffraction

Crystal data

$C_{14}H_{14}ClFeN_5O_8$
Mr = 471.60
Orthorhombic, $C222_1$
a = 9.053 (3) Å
b = 15.456 (6) Å
c = 13.532 (5) Å
V = 1893.5 (11) Å^3
Z = 4
$F(000)$ = 960

D_x = 1.654 Mg m^{-3}
Mo $K\alpha$ radiation, λ = 0.71073 Å
Cell parameters from 625 reflections
θ = 2.6–13.3°
μ = 0.99 mm^{-1}
T = 220 K
Parallelepiped, red
0.03 × 0.02 × 0.02 mm

Data collection

Bruker D8 VENTURE
diffractometer
Radiation source: microsource
φ and ω scans
Absorption correction: multi-scan
SADABS (Sheldrick, V2016/2)
23471 measured reflections

1727 independent reflections
858 reflections with $I > 2\sigma(I)$
R_{int} = 0.383
θ_{max} = 25.4°, θ_{min} = 2.6°
h = −10→10
k = −18→18
l = −16→16

Refinement

Refinement on F^2
Least-squares matrix: full
$R[F^2 > 2\sigma(F^2)]$ = 0.123
$wR(F^2)$ = 0.380
S = 1.06
1727 reflections
126 parameters
1 restraint
Hydrogen site location: inferred from neighbouring sites

H-atom parameters constrained
$w = 1/[\sigma^2(F_o^2) + (0.1929P)^2 + 8.580P]$
where $P = (F_o^2 + 2F_c^2)/3$
$(\Delta/\sigma)_{max} < 0.001$
$\Delta\rho_{max}$ = 0.56 e Å^{-3}
$\Delta\rho_{min}$ = −0.45 e Å^{-3}
Extinction correction: *SHELXL2018*/1 (Sheldrick 2018), $Fc^*=kFc[1+0.001xFc^2\lambda^3/\sin(2\theta)]^{-1/4}$
Extinction coefficient: 0.013 (5)
Absolute structure: Refined as an inversion twin.

Special details

Geometry. All e.s.d.'s (except the e.s.d. in the dihedral angle between two l.s. planes) are estimated using the full covariance matrix. The cell e.s.d.'s are taken into account individually in the estimation of e.s.d.'s in distances, angles and torsion angles; correlations between e.s.d.'s in cell parameters are only used when they are defined by crystal symmetry. An approximate (isotropic) treatment of cell e.s.d.'s is used for estimating e.s.d.'s involving l.s. planes.
Refinement. Refined as a 2-component inversion twin.

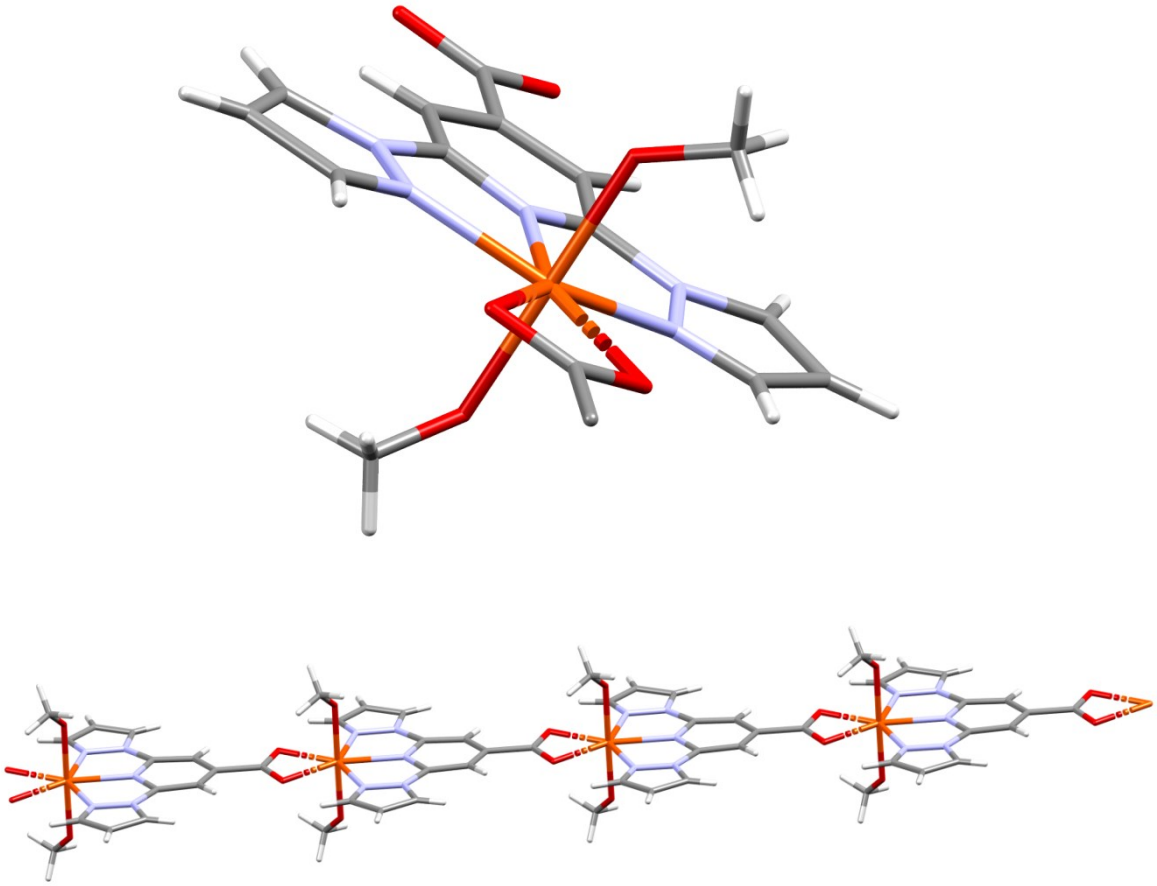

*Figure S22: (top) FeN_3O_4 coordination sphere around Fe(II) in **2** and (bottom) 1D coordination polymer structure of **2**. Color code: Fe=orange, C=grey, N=blue, O=red, H=white.*

The compound **2** is a 1D coordination polymer built with Fe(II) and BPI^- linkers. Each Fe center is coordinated by 3 N atoms from one BPI^- linker, one COO^- group from a second BPI^- linker and 2 MeOH molecules. The electroneutrality of the compound is ensured by the presence of one ClO_4^- counter-anion per Fe site. The average <Fe-N> distance is 2.19Å and the average <Fe-O> distance is 2.18Å, which is consistent with Fe(II) cations in the HS state.

Magnetization measurements

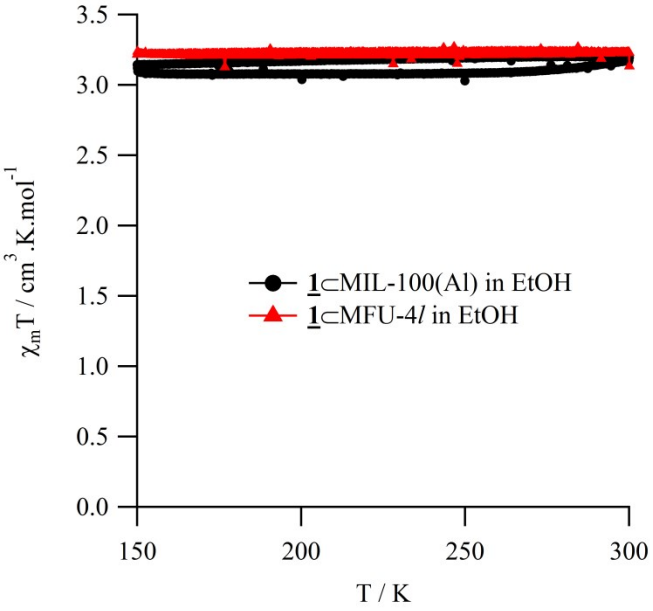

*Figure S23: Evolution of the product of the molar magnetic susceptibility by the temperature vs. temperature for **1**⊂MFU-4l and **1**⊂MIL-100(Al) dispersed in EtOH. The data were normalized taking into account the formula determined by the combination of EDS and NMR spectroscopy.*